



OPEN

Biofabrication of silver nanoparticles with antibacterial and cytotoxic abilities using lichens

Mona A. Alqahtani¹, Monerah R. Al Othman¹ & Afrah E. Mohammed²✉

Recently, increase bacterial resistance to antimicrobial compounds issue constitutes a real threat to human health. One of the useful materials for bacterial control is silver nanoparticles (AgNPs). Researchers tend to use biogenic agents to synthesize stable and safe AgNPs. The principal aim of this study was to investigate the ability of lichen in AgNPs formation and to find out their suppression ability to MDR bacteria as well as their cytotoxic activity. In the current study, lichens (*Xanthoria parietina*, *Flavopunctelia flaventior*) were collected from the south of the Kingdom of Saudi Arabia. Lichens methanolic extracts were used for conversion of Ag ions to AgNPs. Prepared biogenic AgNPs were characterized by Ultraviolet–Visible (UV–Vis) Spectroscopy, Transmission electron microscopy (TEM), Dynamic Light Scattering (DLS) and Zeta potential and Energy-Dispersive X-ray Spectroscopy (EDS). Lichens secondary metabolites were determined by Fourier-Transform Infrared Spectroscopy (FTIR) and Gas Chromatography–Mass Spectrometry (GC–MS). The antibacterial activity and synergistic effect of AgNPs were evaluated against pathogenic bacteria, including gram-positive; Methicillin-resistant *Staphylococcus aureus* (MRSA), Vancomycin-resistant *Enterococcus* (VRE), and gram-negative; (*Pseudomonas aeruginosa*, *Escherichia coli*) as well as the reference strains (ATCC) using the agar disk diffusion method. Cytotoxic effect of biogenic AgNPs was tested against HCT 116 (Human Colorectal Cancer cell), MDA-MB-231 (Breast cancer cell), and FaDu (Pharynx cancer cell) by MTT test. TEM imaging showed well-dispersed spherical particles of 1–40 nm size as well as zeta size showed 69–145 nm. Furthermore, FTIR and GC–MS identified various lichen chemical molecules. On the other hand, the highest antibacterial activity of AgNPs was noticed against *P. aeruginosa*, followed by MRSA, VRE, and *E. coli*. AgNPs influence on gram-negative bacteria was greater than that on gram-positive bacteria and their synergistic effect with some antibiotics was noted against examined microbes. Moreover, higher cytotoxicity for biogenic AgNPs against FaDu and HCT 116 cell line in relation to MDA-MB-231 was noted. Given the current findings, the biogenic AgNPs mediated by lichens had positive antibacterial, synergistic and cytotoxic powers. Therefore, they might be considered as a promising candidate to combat the multi-drug resistance organisms and some cancer cells.

Recently, development of bacterial resistance to antibiotics and related issues constitutes a real threat to human health. In view of public health, new antimicrobial compounds with varied range of activities have to be improved and developed to minimize the resistance of bacteria¹. The World Health Organization (WHO) has issued a universal antimicrobial resistance map, giving alert that the world will soon suffer from a ‘post-antibiotic’ phenomenon. Recently, resistant bacteria for drugs showed great concern because they developed quickly and spread around the world according to (WHO) report²; consequently, there is an urgent need to develop alternatives. In the strictest sense, organism resist multi antimicrobial compounds in vitro is defined as Multi-Drug Resistant (MDR) organisms³. Antibiotic resistance is considered as one of the strongest potential factors in severely infected patients together with the virulence of pathogen resulting in sickness and mortality⁴. Both bacterial types (Gram-positive and Gram-negative) assumed to exhibit resistance to antimicrobial agents. However, gram-negative bacteria with multi-drug resistant ability require special attention. Since such a problem grows continually therefore, searching for solutions and recommendations for proper microbial treatment are needed^{5,6}. Excessive uptake

¹Department of Biology and Microbiology, Faculty of Science, King Saud University, P.O. Box 22452, Riyadh 11495, Saudi Arabia. ²Department of Biology, College of Science, Princess Nourah Bint Abdulrahman University, P.O. Box 84428, Riyadh 11671, Saudi Arabia. ✉email: AFAMohammed@pnu.edu.sa

of antibiotics might lead to adaptational resistance and using of wide-spectrum agents could assist in extending the resistance cycle. These factors have participated in the development of resistance as well as the outbreak of multi-drug resistant organisms^{7,8}. The gradual emergence of bacterial resistance poses a hazard to public health therefore, it is essential to be investigated in a trial to find out reasonable solution. Silver is one of the most important metals that inhibits the growth of microbes; it has been used in ancient times for therapeutic purposes. The high reactivity of silver ions for protein binding, could be the main reason for changes appear in the structure of cell wall and membrane of bacteria resulting in cell death⁹. Using this metal in its natural state has adverse effects on the human body. The human body absorbs silver and silver compounds by ingestion, inhalation, or exposure through the skin or mucous membranes and deposited in small amounts in the kidneys and liver¹⁰. Therefore, converting silver to another form might be required. One of the useful materials for infection control is Silver nanoparticles (AgNPs) which are characterized by small size, a property which offers them unique physicochemical features that differ from their bulk materials, which is basically attributed to greater ratio between their surface area and volume¹¹. Generally, nanotechnology is a base of novel applications such as nanomaterials, nanometrology, electronics, optoelectronics, nanobiotechnology and industrial applications^{12,13}. In particular, AgNPs have been used as delivery tool in gene and colon cancer therapies^{14,15} as well as antibacterial activities^{16–18}. Therefore, AgNPs could be a promising approach to treat MDR because it is rarely to find microbes that resist AgNPs since microbes need various mutation to develop such phenomenon¹⁹ because of metals several targets in microbe²⁰. Recently, researchers tend to use biogenic agents such as plant extracts to synthesize stable AgNPs by treating the aqueous solution of AgNO₃ with the plant extracts as reducing agents²¹. Plant and plant-derived materials are rich in secondary metabolic substances like polysaccharides, vitamins, and proteins. Therefore, it might be the right choice for the biosynthesis of metal nanoparticles²². In the current study, different lichen types were used as biogenic mediators for nanoparticles formation. Lichens are a symbiotic self-sustaining group formed by fungi and algae that have been utilized in the form of medicines, diet and feed, perfumes, spices, and for a variety of purposes¹⁰. Lichens medical application depends on its containing uniquely different active biological substances; to date, about 1050 bioactive ingredients were recognized²³. Lichen active compounds showed diversified types of biological actions containing antioxidant, antimicrobial, cytotoxic, phytotoxic, wound healing, enzyme inhibitory, antiherbivore, analgesic, anti-termite, anti-inflammatory, and others²⁴. Researchers used different types of lichens for AgNPs formation as [*Parmeliopsis ambigua*, *Punctelia subrudecta*, *Evernia mesomorpha*, *Xanthoparmelia plitti*²⁵, *Parmotrema praesorediosum*²⁶, *Cetraria islandica*²⁷, *Ramalina dumeticola*²⁸, *Usnea longissima*¹⁷, *Parmelia perlata*²⁹, *Parmotrema tinctorum*³⁰, and *Cladonia rangiferina*³¹]. However, information about *Xanthoria parietina* and *Flavopunctelia flaventior* usage in AgNPs formation is lacking. Therefore, the aim of the current study was to report such species for the first time as bio mediators in AgNPs formation. In the current study, selected lichen types were collected from the south of the Kingdom of Saudi Arabia and applied as mediator for the conversion of Ag ions to AgNPs. Biogenic AgNPs were characterized using UV–Vis Spectroscopy, TEM, DLS, Zeta potential, and EDS. Lichens Secondary metabolites were determined by FTIR and GC–MS. The antibacterial activity of AgNPs and their synergistic potential with antibiotics were evaluated against pathogenic bacteria, including gram-positive; (MRSA, VRE) and gram-negative; (*P. aeruginosa*, *E. coli*) as well as ATCC of the same bacteria using the agar disk diffusion method. Cytotoxic effect of biogenic AgNPs was tested against HCT 116 (Human Colorectal Cancer cell), MDA-MB-231 (Breast cancer cell), and FaDu (Pharynx cancer cell) by MTT assay.

Materials and methods

Materials. Silver nitrate was purchased from Saudi Overseas Marketing and Trading Company (SOMATCO), Riyadh, Saudi Arabia. For the antibacterial assays, Blood agar, Mueller–Hinton Agar (MHA), and Mueller–Hinton Broth (MHB) was purchased from Saudi Prepared Media Laboratory (SPML) Company, Riyadh, Saudi Arabia. All the clinical isolates and American Type Culture Collection (ATCC) bacteria were obtained from Microbiology Laboratory in King Faisal Specialist Hospital & Research Centre (KFSH&RC), Riyadh, Saudi Arabia. Antibiotic discs were from OXOID; Tetracycline 30 µg for *S. aureus*, Linezolid 30 µg for *E. faecium*, Gentamicin 10 µg for *P. aeruginosa* and Ampicillin 10 µg for *E. coli*. Such appropriate antibiotics for ATCC bacteria were selected by antibiotic disc quality control laboratory reports.

Lichens collection. Lichens samples were collected from Al-Soudah and Bani Mazin Which are mountainous areas at an altitude of about 2900 m of Abha city, South of Saudi Arabia in august 2017, 2018 (Fig. 1). Samples collected at temperature of 19 °C, rainy weather, and foggy is clear in (Fig. 2). During samples collection, some points were taken into consideration, growth form, thallus intact and the margins visibility. Two lichen samples were collected from the trees, thereafter, samples were purified and segregated according to their growth forms and the type of fruiting bodies [Apothecia, Perithecia, Sterile -stretched apothecia lirellae-]³² as shown in Figs. 3, 4. The lichens were washed using distilled water to remove surface impurities and extraneous materials. Then lichen samples were air-dried at room temperature for three days then ground by a grinder to a fine powder. The samples were kept in containers for further usage.

Methods

Identification of lichen samples. Lichen type *Xanthoria parietina* 'Xa' and type *Flavopunctelia flaventior* 'Ff' were identified by morphological, anatomical characters, and chemical tests. The spot test was carried out by direct application of the reagents such as Reagent 10% potassium hydroxide (K), Reagent calcium hypochlorite (C), Reagent (KC), Reagent (Pd) "Steiner's solution"³². Identified samples are presented in Fig. 3 for (Xa) and in Fig. 4 for (Ff), both samples were early found and documented in Saudi Arabia³³.



Figure 1. The location of collected lichen.



Figure 2. Habitat of collected lichens.



Figure 3. Lichen type *Xanthoria parietina* on the tree (left) and after cleaning (right).



Figure 4. Lichen type *Flavopunctelia flaventior* on the tree (left) and after cleaning (right).

Extraction of lichens. An alcohol extract of each lichen was prepared by mixing 10 g of a lichen powder with 100 mL of 80% methanol. The mixtures were left shaking (160 rpm for 24 h) at room temperature. Then mixture was filtered through 'Whatman filter paper Grade 1' and further filtered through 'Whatman filter paper Grade 3' for more extract purification then kept at 4 °C. Furthermore, 100 mL methanol was added to the rest of the extract and left more 24 h on the shaker under the same previous conditions. The mixture was filtered twice in the same way as before and the methanol was removed by a rotary evaporator device. The round bottom flask was weighed before and after extraction, then the difference was calculated, the concentration of the final extract was 10 mg/mL. The extract was closed tightly and saved at 4 °C until used³⁴.

Optimization of AgNPs synthesis conditions. The parameters that may affect the nanoparticles biosynthesis were tested such as the ratio of lichen extract to AgNO₃ solution was tested according to (1:9, 1:3, 1:2, 1:1), AgNO₃ concentration (1 mM, 10 mM), incubation time (24 h, 48 h, 72 h) and temperature degree (25 °C; 40 °C). After the color change, the particle size was measured by zetasizer. Thereafter, AgNPs were synthesized by application of the conditions that provided small particle size²⁷ and considered as an optimum conditions. AgNPs prepared using *Xanthoria parietina* is known as Xa-AgNPs and those prepared using *Flavopunctelia flaventior* are Ff-AgNPs.

Synthesis of AgNPs. For the synthesis of the AgNPs, about 5 mL of the methanol extract of lichen (10 mg/mL) were mixed with 15 mL of AgNO₃ (10 mM) solution in a flask and shaken for 3:30 h under dark conditions then allowed to react at 40 °C for 72 h²⁷.

Characterization of biogenic AgNPs. Different methods for the characterization of the biogenic AgNPs prepared in the current study were used for nanoparticles description such as:

Ultraviolet–Visible Spectroscopy. Ultraviolet–Visible (UV–Vis) Spectroscopy absorption was measured using a spectrophotometer (BIOCHROM Libra S60PC, Serial Number: 119377, England). All measurements were performed for the mixture after 24 h of reaction within the range of 300–600 nm and deionized water was used as a blank²⁵.

Transmission electron microscopy (TEM). The size distribution and morphology of AgNPs were investigated at 80 kV voltage by TEM (JEM-1011, JEOL, Japan). samples were prepared by drop-coating on carbon-coated (200 mesh) TEM grids²⁶.

Dynamic Light Scattering (DLS) and Zeta potential. The size distribution pattern was evaluated by a dynamic light scattering technique and the electrical charge of particles by zeta potential were the measurement with a Zetasizer (NANO ZSP, Malvern Instruments Ltd, Serial Number: MAL1118778, ver 7.11, UK) according to Sid-diqi et al.¹⁷.

Energy-dispersive X-ray spectroscopy (EDS). EDS was used for the elemental analysis and confirmed the presence of the silver element precisely using SEM (JEOL, JED-2200 series, Japan)³⁵.

Fourier-transform infrared spectroscopy (FTIR). FTIR measurements were carried out to identify the potential biomolecules in lichen extract responsible for reducing and capping the reduced AgNPs. The spectra were

Cell line	Tissue	Disease
HCT 116	Colon	Colorectal carcinoma
MDA-MB-231	Mammary gland/breast	Adenocarcinoma
FaDu	Pharynx	Squamous cell carcinoma

Table 1. Cancer cell lines information. Organism: human; morphology: epithelial; culture properties: adherent.

recorded on FTIR spectroscopy (SPECTRUM100, Perkin-Elmer, USA) using a diffuse reflectance accessory, and the scanning data were obtained with a range between 450–3500 cm^{-1} ²⁷.

Identification of Lichens Secondary metabolites by (GC–MS). The Gas chromatography-mass spectrometry (GC–MS) analyses of lichens methanol extracts were conducted by using (AGILENT Technologies 220 Ion Trap GC/MS, USA). Helium was used as the carrier gas with column (Flow rate 1 mL/min; Pressure 8.2317 psi; Average Velocity 36.623 cm/s; Holdup Flow 1.3653 min; Post run 0.99996 mL/min; 450 °C: 30 m \times 250 μm \times 0.25 μm). The injector and interface were operated at 250 °C; Initial oven temperature was 70 °C to finally programmed to 250 °C with run time is at 52 min. The compounds of lichen extracts were analyzed using the National Institute of Standards and Technology (NIST) chemical database^{36,37}.

Evaluation of antibacterial activity of AgNPs. *Antibacterial susceptibility testing (AST).* The antibacterial activity of AgNPs was evaluated against four pathogenic bacteria including two gram-positive (MRSA, VRE), and two gram-negative (*P. aeruginosa*, *E. coli*) as well as the reference strains using the agar disk diffusion method. Pure cultures of each strain were sub-cultured on blood agar plates and grown for 24 h at 37 °C. By direct colony suspension method, McFarland standard 0.5 bacterial suspensions (1.5×10^8 CFU/mL) in the saline tube was prepared using McFarland reader. MHA plates were inoculated by tested strains using a petri plate rotator. The sterile discs were saturated by 20 μL of AgNPs and kept for drying under aseptic conditions. Then dried discs were transported to bacterial cultured agar surface using sterile forceps with pressure for the discs to be closely bonded. Sterile distilled water was used as negative control and antibiotic susceptibility discs were used as positive controls. After 15 min of discs application, plates were inverted and incubated at 35 °C for 16–18 h according to the Clinical and Laboratory Standards Institute³⁸. The zone of inhibition around the discs was measured by Vernier caliper. Antibacterial activity was investigated and zone diameter breakpoints (mm) for antibiotics were determined according to M02 and M07 from^{39,40}. Such mentioned methods were also applied for lichen methanol extracts and methanol was used as positive control²⁶.

MICs and MBCs determination. The minimal inhibitory concentrations (MICs) of the AgNPs were determined by the microdilution method in 96-well microtiter plates. The obtained concentration range of lichen extract was from 2.5 to 0.0098 mg/mL. Positive control (media contains inoculum with antibiotic), negative control (media contain inoculum), and AgNPs solution (media with AgNPs) was applied in the last three columns. All plates were incubated for 18–20 h at 35 °C. MICs were determined by comparing to positive and negative control wells. The lowest concentration with no growth (turbidity or pellet) was defined as MICs. Results expressed as the mean values of two independent replicates. MICs breakpoints ($\mu\text{g/mL}$) for antibiotics was determined by CLSI^{39,40}. The minimum bactericidal concentrations (MBCs) was determined from broth microdilution by sub-culturing a sample from wells on MHA plates by loop 1 μL . After 24 h of plates incubation, the concentration that kills 99.9% of bacterial growth has been defined as MBC⁴¹. Furthermore, the tolerance level was calculated as MBCs/MICs ratios to find-out the expected action for AgNPs (bactericidal or bacteriostatic) against tested bacteria¹⁶.

Synergistic effect of AgNPs and antibiotics against MDR pathogens. The disk diffusion method was used to test the effect of antibiotics in combination with AgNPs against the MDR bacteria. Test plates were inoculated with the microbes in the same way as AST. AgNPs at concentration of 20 μg was added to each disc of Tetracycline (TE), Linezolid (LZD), Gentamicin (CN), and Ampicillin (AMP), then transported to bacterial cultured agar to test the prepared discs activities. Antibiotic discs were used as positive control. The plates were incubated for 18 h at 35 °C⁴² then the inhibition zone around discs were assessed.

Cytotoxicity of AgNPs. *Cell lines.* HCT 116, MDA-MB-231 and FaDu were used (Table 1). All cells were grown in GIBCO Dulbecco's modified Eagle's medium (DMEM) which containing 10% fetal bovine serum (FBS), 2 mM glutamine, 100 U penicillin and 0.1 mg/mL streptomycin. Culture flasks were incubated for 4 days at 37 °C, 99–100% humidity in 5% CO_2 incubator. The subculture of cells was performed daily to keep the cells from over confluent. After four days of incubation, the media was removed from cell culture flasks T-25 using a sterile pipette. The cells were washed by 5 mL phosphate buffer saline (PBS) for 1 min then added to 1 mL of trypsin. After 2 min, culture flask was checked under the microscope for cells detachment from substrate. 2 mL of media was added to the flask to stop the reaction because the FBS inactivated the trypsin. The cells were placed in tubes and centrifuged for 5 min 6000 rpm to dispose of the trypsin. 2 mL of the medium was put for precipitation then the number of cells was counted⁴³.

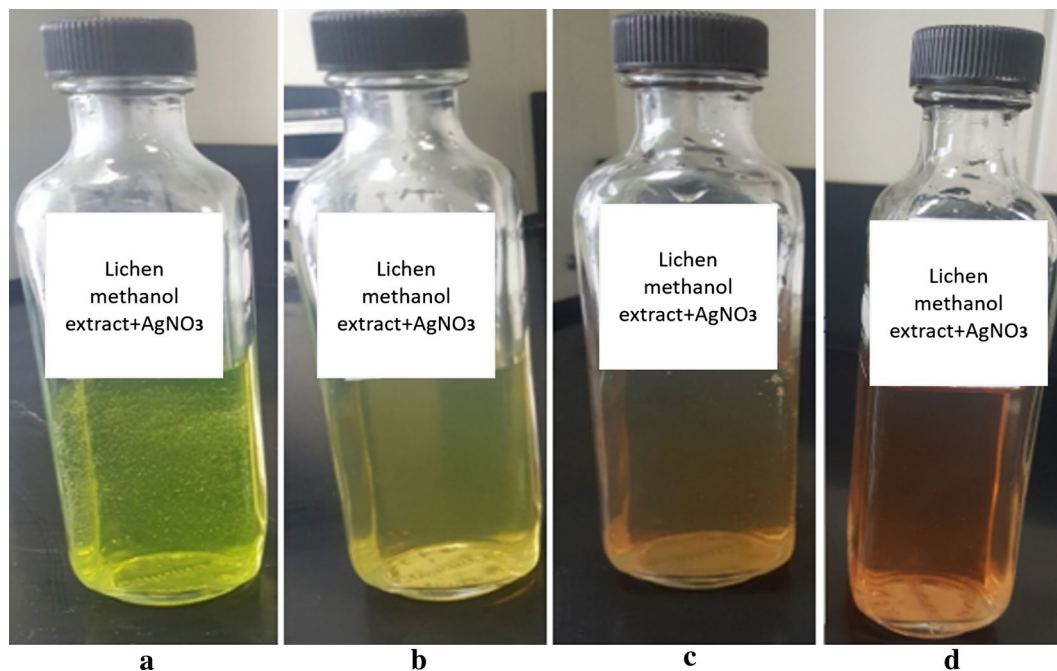


Figure 5. Color change during the reaction time for during Xa-AgNPs preparation, where (a) is indicating the colour immediately after mixing, (b) after 24 h, (c) after 48 h and (d) is the colour after 72 h.

Cells count. A ratio of 1:2 cell culture contains 50 μL and 50 μL of Trypan Blue Solution (0.4%) in Eppendorf tube was added and injected in cell counting slide at rate of 20 μL for each side. The slide was entered in (LUNA automated cell counter; Logos Biosystems, Gyunggi-do, Korea). Serial dilutions of cells in media were prepared to obtain cell count (5×10^4) cells/mL^{43,44}.

Application of AgNPs on cell culture (Microplate 96-well). 100 μL of media in (Dilution plate) was added for each well except first and last row due to its exposure to air more than the internal rows. 50 μL of Xa-AgNPs was placed in the first well of the second and third row. 50 μL of lichen extract (Xa) was placed in the first well of the fourth and fifth row. 50 μL of methanol was placed in the first well of the sixth and seventh row and methanol was used as control. Using serial dilution method by multichannel micropipette; 50 μL was transferred from the first column to the second column and so on to last column and disposal of the rest 50 μL . 120 μL of cell suspension in cultivation plate was added to each well except first and last row. 60 μL of each column in dilution plate was transferred to the same column in cultivation plate; More precisely 60 μL of (tested material with media) was transferred from the last column of dilution plate to last column of cultivation plate (from lowest concentration to the highest concentration), and so on with all columns. These methods were applied to Ff and Ff-AgNPs and the experiment was performed in duplicate³⁵.

MTT assay. 250 mg of MTT 3-(4,5-dimethylthiazol-2-yl)-2,5-diphenyl tetrazolium bromide was dissolved in 50 mL of PBS and stirred with a magnetic stirrer for homogenization. 20 μL of MTT was added to each well then incubated for 2 h at 37 $^{\circ}\text{C}$, 99–100% humidity in 5% CO_2 incubator. The medium was removed by suction. Cells were washed with PBS and centrifuged to removed dead cells and cellular debris. 100 μL of isopropanol ($\text{C}_3\text{H}_8\text{O}$) was added to each well then was shaken for 10 min. MTT conversion to purple-colored formazan crystals is due to presence of viable cells with active metabolism. Absorbances were measured at 595 nm by ELISA reader (ANTHOS 2010 Microplate Reader, Biochrom LTD, UK). The cell viability was calculated using following formula:

$$\text{Cell viability } 100\% = (\text{OD Sample}/\text{OD Control}) \times 100.$$

Half-maximal inhibitory concentration (IC_{50}) values represent the concentration of tested materials that required for 50% inhibition of cells growth. IC_{50} values were measured from the regression curves⁴⁵.

Statistical analysis. Means and standard deviations for antibacterial activities were calculated using MICROSOFT EXCEL 2019. AgNPs images were chosen as one of the triplicates. ORIGIN software version 6.1 (ORIGIN Lab Corporation, Northampton, USA) statistical analyses was used for MTT assay for IC_{50} assessment.

Results

Biosynthesis of AgNPs. To obtain the best AgNPs size, conditions were optimized and adjusted as follows: the two lichen types were extracted by methanol and each extract was added to AgNO_3 (10 mM) at a ratio of 1:3 at 40 $^{\circ}\text{C}$ for 72 h. It was noticed that increasing the reaction temperature and AgNO_3 concentration reduced

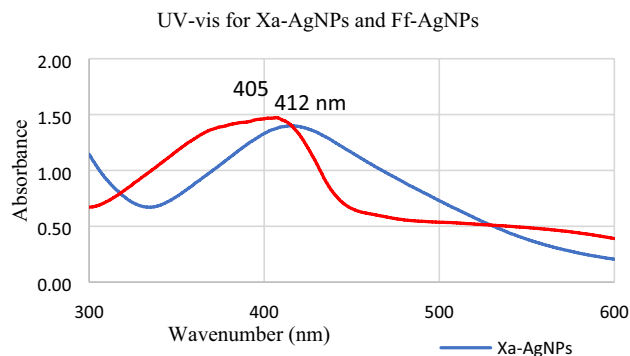


Figure 6. UV–Vis for Xa-AgNPs and Ff-AgNPs.

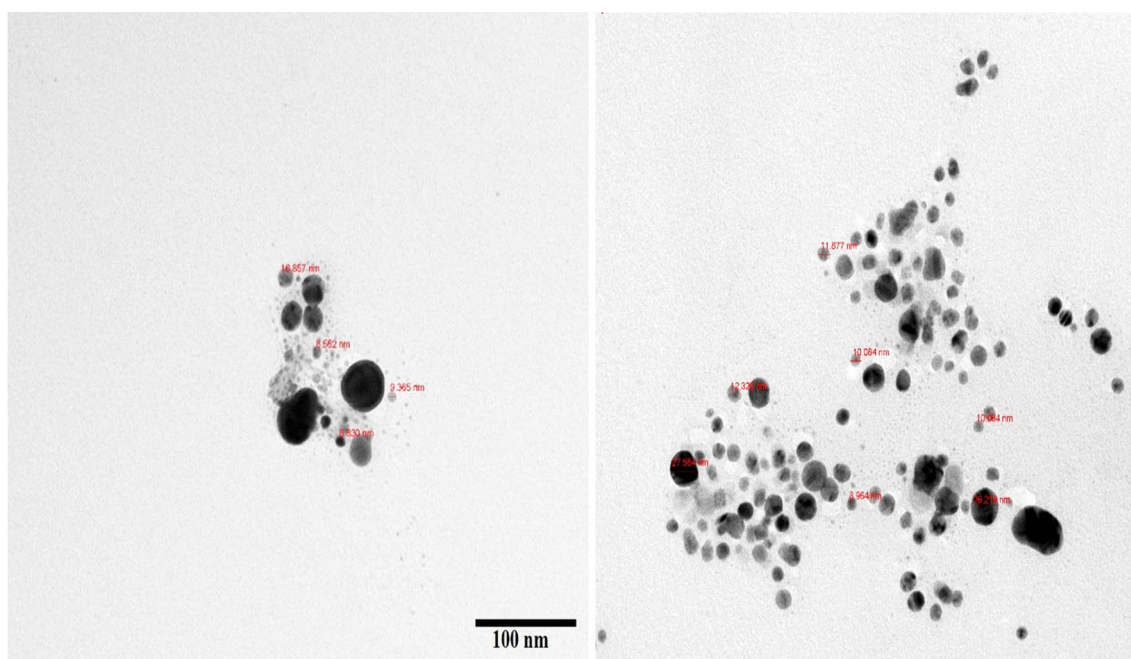


Figure 7. TEM images for Xa-AgNPs (left) and Ff-AgNPs (right).

the reaction time since conversion time of Ag ions to AgNPs at 40 °C for AgNO₃ at 10 mM concentration was shorter when compared to that at 25 °C and 1 mM. The reaction mixture immediately assumed yellow green colour for Xa-AgNPs (Fig. 5) which was then started to change gradually after 24 h in time dependant manner. After 72 h, the mixture was turned to brown and no more colour changes were noted. Such colour stability might point to attainment of maximum reduction time but also it revealed that, colour intensity was highly time dependant. both Xa-AgNPs and Ff-AgNPs assume similar pattern in colour development and stable nanomaterials for more than 4 months were approved.

Characterization of biogenic AgNPs. Reactions between silver ions and both lichen extracts were monitored by UV–Vis Spectroscopy of AgNPs (Fig. 6). The analysis of UV–Vis spectroscopy showed an appearance of surface plasmon resonance peak at 412 and 405 nm for Xa-AgNPs and Ff-AgNPs respectively. TEM imaging for Xa-AgNPs and Ff-AgNPs showed well-dispersed spherical particles of 1–40 nm size, furthermore, clear capping agents around AgNPs as light colour were detected (Fig. 7). Results obtained from DLS for Xa-AgNPs and Ff-AgNPs had average diameters of 145 and 69 nm with a polydispersity index (PDI) of 0.291 and 0.458, respectively (Fig. 8). Zeta Potential values were – 24, – 20 mV (Fig. 9) for Xa-AgNPs and Ff-AgNPs respectively. Analysis through EDS confirmed the presence of the silver element in both AgNPs beside the carbon and oxygen. The results showed strong silver signals Ag-L at 3 keV, along with carbon peak and oxygen peak (Fig. 10). FTIR spectra characterized the lichen extracts from ‘Xa and Ff’ as well as after AgNPs prepared by their aid (Fig. 11). Absorbance peaks for both lichen types were at 3421 cm⁻¹, 2066 cm⁻¹, 1634 cm⁻¹ and 593 cm⁻¹. Additionally, the absorbance peaks for Xa-AgNPs and Ff-AgNPs were at 3421–3332 cm⁻¹, 2070 cm⁻¹, 1637 cm⁻¹, and 541 cm⁻¹, representing the role of various functional groups in the bio-reduction of AgNO₃.

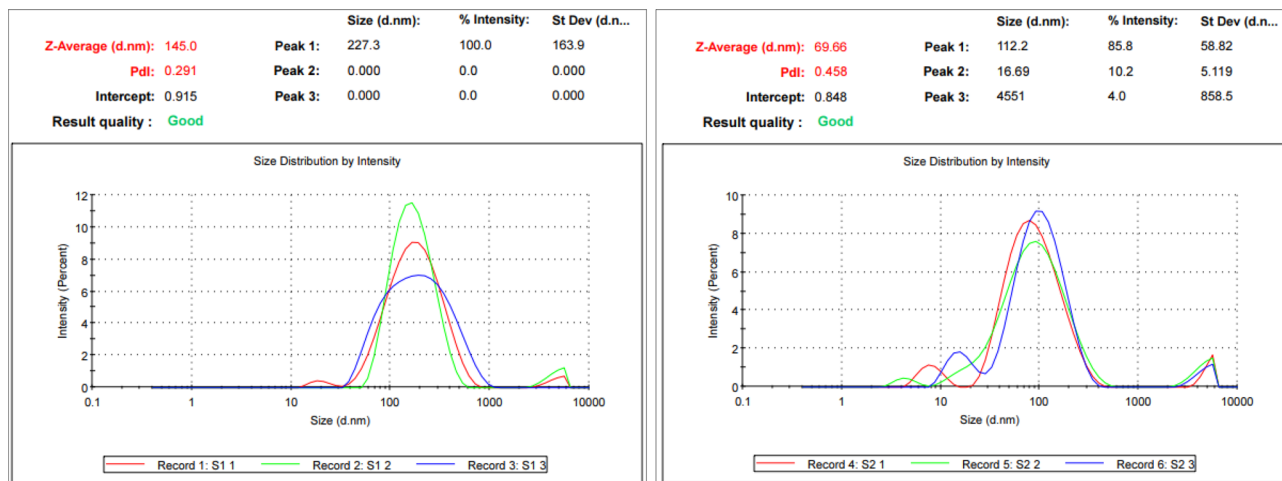


Figure 8. Particles size of Xa-AgNPs (left), Ff-AgNPs (right).

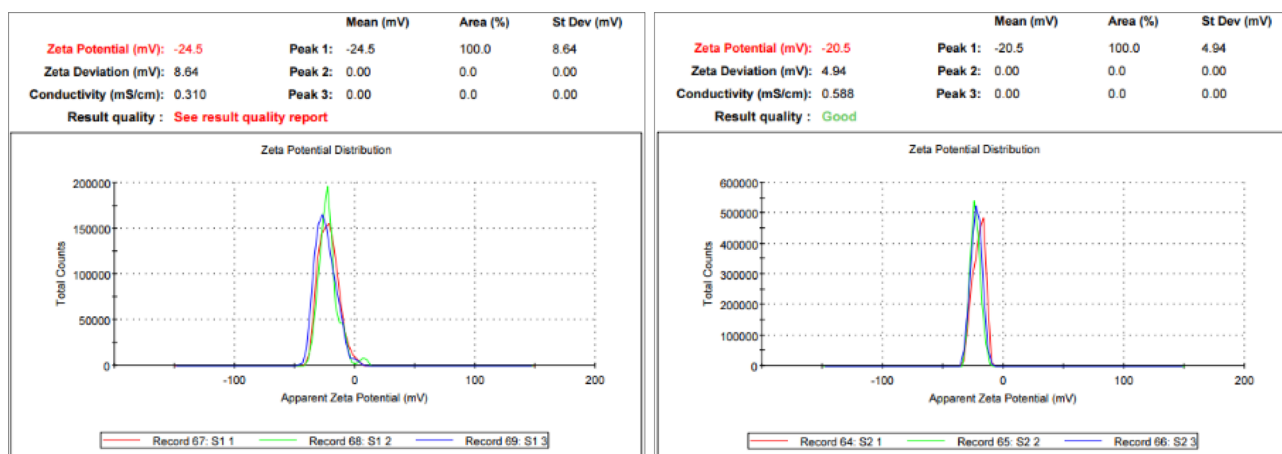


Figure 9. Zeta Potential of Xa-AgNPs (left), Ff-AgNPs (right).

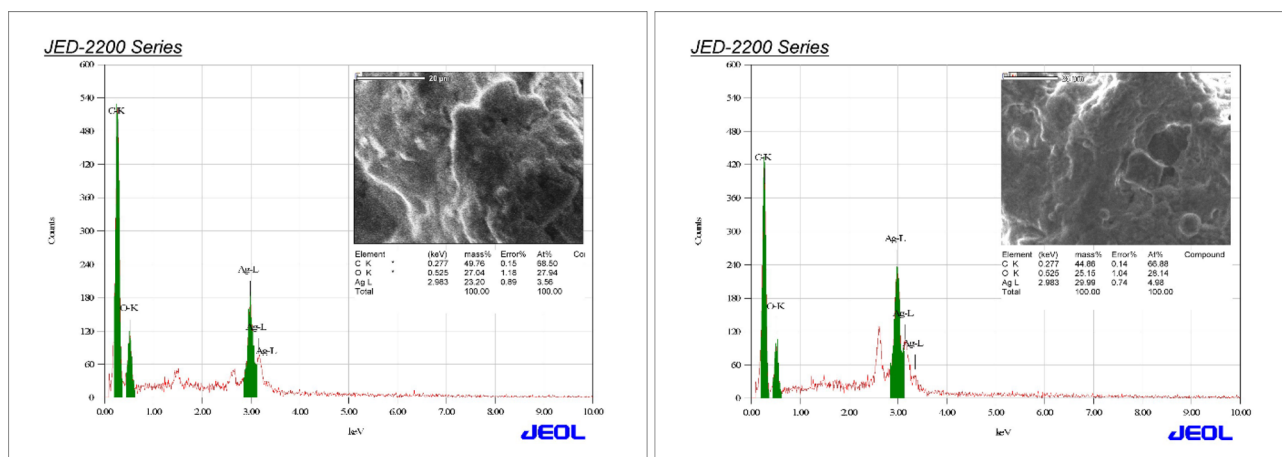


Figure 10. EDS for Xa-AgNPs (left), Ff-AgNPs (right).

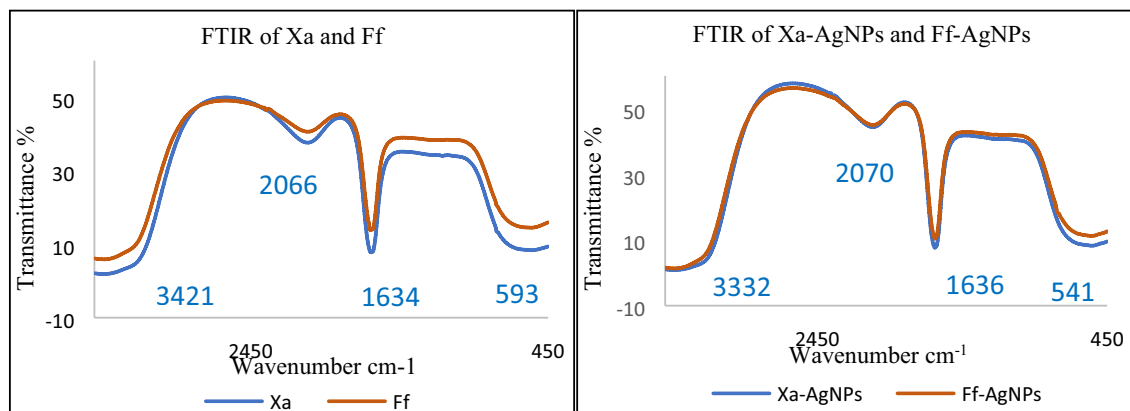


Figure 11. FTIR for lichen extracts Xa and Ff (left) and that for Xa-AgNPs and Ff-AgNPs (right).

Name	Formula	Molecular weight	Retention time	Found in lichen	Nature of compounds
Benzyl bromide	C ₇ H ₇ BrO	171	0.713	Xa	Benzyl Halide
2-Amino-2-ethyl-1,3-propanediol	C ₅ H ₁₃ NO ₂	119	2.279	Xa	Alkanolamine
Dichloran	C ₆ H ₄ Cl ₂ N ₂ O ₂	206	26.187	Xa	Nitroaniline
Hexachlorophene	C ₁₃ H ₆ Cl ₆ O ₂	406	1.480	Xa	Phenolic
Pyrrolidine, 1-methyl-	C ₅ H ₁₁ N	85	1.742	Xa	Alkaloid
undecanal	C ₁₁ H ₂₂ O	170	7.2653	Xa	Fatty aldehyde
Benzenamine, 4-methoxy-N-methyl-	C ₈ H ₁₁ NO	137	13.500 13.515	Xa, Ff	Amine -Aniline
2,5-Cyclohexadiene-1,4-dione, 2,6-bis(1,1-dimethylethyl)-	C ₁₄ H ₂₀ O ₂	220	26.172	Ff	Benzoquinone
2',5'-Dihydroxypropiophenone	C ₉ H ₁₀ O ₃	166	22.039	Ff	Phenolic
3,4-Dimethyl-2-hexanone	C ₈ H ₁₆ O	128	7.245	Ff	Ketone
Acetaldehyde, methylhydrazone	C ₃ H ₈ N ₂	72	31.704	Ff	Methyl-hydrazine
Atropine	C ₁₇ H ₂₃ NO ₃	289	14.386	Ff	Alkaloid
Beclomethasone	C ₂₂ H ₂₉ ClO ₅	408	1.493	Ff	Corticosteroid
Butanenitrile 3-methyl-	C ₅ H ₉ N	83	1.847	Ff	Nitrile
Colchicine	C ₂₂ H ₂₅ NO ₆	399	37.123	Ff	Alkaloid
Cortisone	C ₂₁ H ₂₈ NO ₅	360	44.087	Ff	Corticosteroid
Cyclopentadecanol	C ₁₅ H ₃₀ O	226	24.798	Ff	Alcoholic
Cyclopentanone, oxime	C ₅ H ₉ NO	99	2.277	Ff	Hydroxyl-amine
Dehydrocholic acid	C ₂₄ H ₃₄ O ₅	402	34.141	Ff	Cholagogue and Choleric
Hydrocortisone acetate	C ₂₃ H ₃₂ O ₆	404	33.827	Ff	Steroid
Isobutane	C ₄ H ₁₀	58	1.710	Ff	Alkane
Octadecanamine	C ₁₈ H ₃₉ N	269	36.685	Ff	Amine
Oxacyclododecan-2-one	C ₁₁ H ₂₀ O ₂	184	7.262	Ff	Fatty ester
Piperidine	C ₅ H ₁₁ N	85	1.737	Ff	Alkaloid
Ricinoleic acid	C ₁₈ H ₃₄ O ₃	298	21.246	Ff	Fatty acyls—octadecanoid

Table 2. GC–MS analysis of lichen *Xanthoria parietina* ‘Xa’ and *Flavopunctelia flaventior* ‘Ff’.

Identification of Lichens secondary metabolites by (GC–MS). To find out the chemical constituents that could be involved in conversion of silver ions to AgNPs, Gas chromatography–mass spectrometry was used for lichen methanol extracts. GC–MS analysis of both lichen types showed the presence of 25 compounds (Table 2). Benzenamine, 4-methoxy-N-methyl-compound was noticed for both lichen types.

Evaluation of antibacterial activity of AgNPs. The antibacterial activities of lichen extracts and the biogenic AgNPs were evaluated against MDR and ATCC bacterial strains. No antibacterial activity was detected for lichen extracts however, AgNPs inhibited the growth of both tested gram-negative and gram-positive strains (Table 3). The highest antibacterial activity of Xa-AgNPs and Ff-AgNPs was noticed against *P. aeruginosa* followed by MRSA, VRE and *E. coli*, respectively. No significant variations were observed in the activity of Xa-AgNPs and Ff-AgNPs against tested ATCC and MDR bacteria. MRSA, VRE, *P. aeruginosa* MDR, and *E. coli* ATCC were more sensitive of Ff-AgNPs compared to Xa-AgNPs. Furthermore, the MICs and MBCs of Xa-

The diameter of the zone of inhibition of AgNPs (mm) at (5 mg/mL)				
Bacteria strains	Xa-AgNPs ^a that size 145	Ff-AgNPs ^a that size 69	AgNO ₃	(+) Control 'Antibiotics'
MRSA	11.3 ± 0.2	11.8 ± 0.2	6.3 ± 0.5	TE30: 18 ± 0
<i>S. aureus</i> ATCC	12.3 ± 0.2	11.6 ± 0.5	6.8 ± 0	TE30: 21 ± 0
VRE	10.1 ± 0.2	10.3 ± 0.2	5.1 ± 0.2	LZD30: 21 ± 0
<i>E. faecium</i> ATCC	10.1 ± 0.2	10.3 ± 0.2	5 ± 0.2	LZD30: 24 ± 0
<i>P. aeruginosa</i> MDR	13 ± 0	13.5 ± 0.5	6.3 ± 0.2	CN10: 11 ± 0
<i>P. aeruginosa</i> ATCC	12.8 ± 0.2	12.5 ± 0.5	6.6 ± 0.5	CN10: 18 ± 0
<i>E. coli</i> MDR	7.6 ± 0.2	7.5 ± 0.5	4.5 ± 0	AMP10: 10 ± 0
<i>E. coli</i> ATCC	7.3 ± 0.5	8.8 ± 0.2	4.3 ± 0.2	AMP10: 20 ± 0

Table 3. Agar disk diffusion assay of Xa-AgNPs and Ff-AgNPs. ^aXa-AgNPs are the AgNPs prepared using *Xanthoria parietina* and Ff-AgNPs are the AgNPs prepared using *Flavopunctelia flaventior*, Methicillin-resistant *Staphylococcus aureus* (MRSA), Vancomycin-resistant *Enterococcus* (VRE), American Type Culture Collection (ATCC), Multi-Drug Resistant (MDR), Tetracycline 30 µg (TE30), Linezolid 30 µg (LZD30), Gentamicin 10 µg (CN10), Ampicillin 10 µg (Amp10). The mean and standard deviation of triplicate were presented in all results.

Bacteria strains	MICs (mg/mL)		MBCs (mg/mL)	
	Xa-AgNPs ^a	Ff-AgNPs ^a	Xa-AgNPs ^a	Ff-AgNPs ^a
MRSA	0.078	0.156	0.312	0.312
<i>S. aureus</i> ATCC	0.078	0.039	0.156	0.078
VRE	0.156	0.078	0.625	0.312
<i>E. faecium</i> ATCC	0.156	0.078	0.625	0.156
<i>P. aeruginosa</i> MDR	0.039	0.019	0.078	0.039
<i>P. aeruginosa</i> ATCC	0.039	0.019	0.156	0.078
<i>E. coli</i> MDR	0.156	0.078	0.312	0.156
<i>E. coli</i> ATCC	0.078	0.039	0.312	0.078

Table 4. MICs and MBCs for the biogenic AgNPs. ^aXa-AgNPs are the AgNPs prepared using *Xanthoria parietina* and Ff-AgNPs are the AgNPs prepared using *Flavopunctelia flaventior*.

Bacteria strains	Xa-AgNPs ^a	Ff-AgNPs ^a
MRSA	4	2
<i>S. aureus</i> ATCC	2	2
VRE	4	4
<i>E. faecium</i> ATCC	4	2
<i>P. aeruginosa</i> MDR	2	2
<i>P. aeruginosa</i> ATCC	4	4
<i>E. coli</i> MDR	2	2
<i>E. coli</i> ATCC	4	2

Table 5. Tolerance level (MBC/MIC) of Xa-AgNPs and Ff-AgNPs. ^aXa-AgNPs are the AgNPs prepared using *Xanthoria parietina* and Ff-AgNPs are the AgNPs prepared using *Flavopunctelia flaventior*.

AgNPs and Ff-AgNPs against tested bacteria were listed in Table 4. The MICs (Lack of turbidity or pellet in the test tube) was observed up to the concentration of 0.019 and 0.039 mg/mL for both biogenic AgNPs against *P. aeruginosa* (MDR and ATCC), while MBCs were recorded at a concentration of 0.078 and 0.039 mg/mL for Xa-AgNPs and Ff-AgNPs, respectively against *P. aeruginosa* MDR. However same MBC was noticed for both AgNPs against *P. aeruginosa* ATCC and *S. aureus* ATCC (Table 4). For tolerance level of AgNPs against tested bacteria, MBCs/MICs ratios were calculated and determined whether AgNPs action were bacteriostatic or bactericidal. Xa-AgNPs and Ff-AgNPs showed bactericidal effect against all tested bacterial strains since the tolerance levels were ≤ 4 (Table 5). In addition, the possible synergistic effect was noted against all tested strains when combination between each of Xa-AgNPs and Ff-AgNPs with antibiotics was done. Results showed clear inhibition zone around the discs for all tested bacterial strains (Fig. 12). Such combination of each Xa-AgNPs and Ff-AgNPs and antibiotics provided efficient activity against MRSA and VRE more than *P. aeruginosa* and *E. coli* (Table 6). Ff-

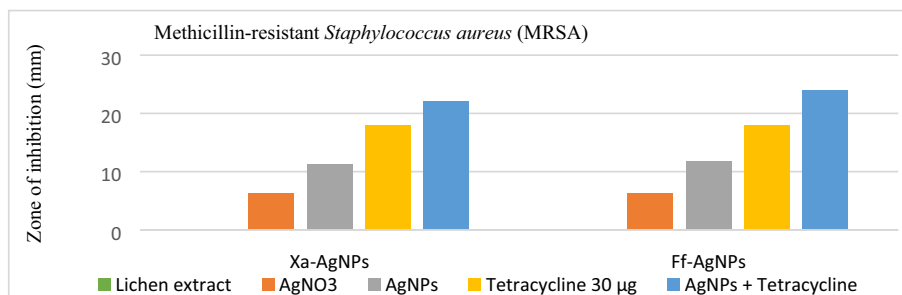


Figure 12. Synergistic effect of Xa-AgNPs and Ff-AgNPs and antibiotics on MRSA.

Diameter of the zone of inhibition of Xa-AgNPs and Ff-AgNPs (5 mg/mL) with antibiotics (mm)			
Bacteria strains	Xa-AgNPs ^a + Antibiotic	Ff-AgNPs ^a + Antibiotic	(+) Control 'Antibiotics'
MRSA	22 ± 0	24 ± 0	TE 30: 18 ± 0
<i>S. aureus</i> ATCC	21.5 ± 0.5	22 ± 0	TE30: 21 ± 0
VRE	26 ± 0	26 ± 0	LZD30: 21 ± 0
<i>E. faecium</i> ATCC	25.1 ± 0.2	27 ± 0	LZD30: 22 ± 0
<i>P. aeruginosa</i> MDR	13 ± 0	13.5 ± 0	CN10: 11 ± 0
<i>P. aeruginosa</i> ATCC	20 ± 0	20 ± 0	CN10: 18 ± 0
<i>E. coli</i> MDR	11 ± 0	11 ± 0	Amp10: 10 ± 0
<i>E. coli</i> ATCC	21 ± 0	20.6 ± 0.5	Amp10: 20 ± 0

Table 6. Synergistic effect of Xa-AgNPs and Ff-AgNPs and antibiotics against bacteria strains. ^aXa-AgNPs are the AgNPs prepared using *Xanthoria parietina* and Ff-AgNPs are the AgNPs prepared using *Flavopunctelia flaventior*.

IC ₅₀ values µg/mL as measured in MTT assay				
Cancer cell lines	Xa-AgNPs ^a (145 nm)	Xa-Extract	Ff-AgNPs ^a (69 nm)	Ff-Extract
MDA-MB-231	250	330	35	40
FaDu	93	170	23	34
HCT 116	96	210	29	38

Table 7. Cytotoxicity of Xa-AgNPs and Ff-AgNPs against Cancer cell lines. ^aXa-AgNPs are the AgNPs prepared using *Xanthoria parietina* and Ff-AgNPs are the AgNPs prepared using *Flavopunctelia flaventior*.

AgNPs increased the efficiency antibiotic TE up to 133% against MRSA, while its activity increased up to 123% against VER when combined with each prepared AgNPs.

Cytotoxicity of AgNPs. Xa-AgNPs and Ff-AgNPs showed higher cytotoxic effect compared to that of lichen extracts 'Xa and Ff' (Table 7). Results from the current study indicated higher cytotoxicity for Xa-AgNPs and Ff-AgNPs against FaDu and HCT 116 cell line in relation to MDA-MB-231. Higher efficiency was observed for Ff-AgNPs compared to Xa-AgNPs.

Discussions

Bioynthesis of AgNPs. The present study could be considered as the first report indicating the biosynthesis of AgNPs by the aid of the extracts of lichen types *Xanthoria parietina* and *Flavopunctelia flaventior* as well as reporting their antibacterial and cytotoxic activities. Interestingly, methanol has the capability of dissolving polar compounds with a polarity index of 5.1. while water has a polarity index of about 10.2²⁹. Our previous study presented the formation of AgNPs by water extract of lichen *Parmotrema clavuliferum*⁴⁶. However, currently methanol was used for extraction of lichens. Optimizing the conditions for fabrication of AgNPs using both lichens tested were confirmed by color change thereafter, particles size average were measured by zetasizer. Factors affected the synthesis of nanoparticles were the ratio of AgNO₃ to lichen extract, AgNO₃ concentration, temperature and reaction time²⁷. Biogenic AgNPs using *Cetraria islandica* formed in few minutes²⁷, 30 min using *Parmelia perlata*²⁹, 24 h using *Parmotrema praesorediosum*²⁶ and 72 h using *Cladonia rangiferina*³¹. It could be concluded that, variations in time needed for nanoparticle formation might likely be related to solvent type, method and conditions of extraction, secondary metabolites of lichens and their concentration. Our findings

were in accordance with the findings of many researchers who reported 1:3 as the ratio of the extract to the silver nitrate, however, they studied aqueous extract of lichens^{26,28–31,35}. Siddiqi, et al.⁴⁷ confirmed that, color intensity of the mixture increased with temperature increment and quick formation of nanoparticles was obtained. The first sign for AgNPs synthesis using lichen extracts was the change of color from yellow-green to dark-brown in the reaction mixture. Such conversion could be a clear indication for the reduction of silver ions to AgNPs which is related to surface plasmon resonance (SPR) phenomenon²⁷. The exact mechanism included in the process of AgNPs formation using biogenic agents was not clearly known, however, several hypotheses of AgNPs formation by the green synthesis was explored in the biological system. The main hypothesis was that, AgNPs are formed underneath the surface of the cell wall and reduced in the presence of biomolecules or enzymes, while intracellular synthesis occurs inside the cells^{17,48}. It has been suggested that the silver ions require nicotinamide adenine dinucleotide (NADH) and NADH-dependent nitrate reductase enzymes⁴⁹. In the case of lichens such enzyme is secreted by the fungal partner extracellularly²⁵ and several secondary metabolites which act as reducing agents to produce AgNPs from AgNO₃ without producing toxic by-product^{28,30}.

Characterization of biogenic AgNPs. The SPR peaks for Xa-AgNPs and Ff-AgNPs corresponded to AgNPs production where AgNPs absorb radiation intensely at a wavelength of 400–450 nm due to the transition of electrons^{25,26}. The peaks at 400 nm are supposed to be as indicators for spherical shapes of the particles¹⁷. TEM analysis confirmed the formation of silver nanostructures and visualized of synthesized AgNPs at 100 nm scales. The morphology and size distribution of both Xa-AgNPs and Ff-AgNPs showed spherical particles with nonspecific distribution. Our TEM findings are well matching with reports in the literature where same size range and spherical particles shape were noted^{17,26–28,30,31}. It was noticeable that the edges of the particles were lighter than the centres, suggesting that bioorganic molecules such as proteins in lichen and other metabolites capped the AgNPs contributed to reduction of Ag ions to AgNPs³⁰. Particle sizes in DLS and Zeta Potential analysis of Xa-AgNPs and Ff-AgNPs with Polydispersity Index (PDI) were in agreement with the particle size early mentioned^{17,30}. Zeta Potential provided high negative value of zeta potential for both AgNPs confirming the repulsion among the particles, and the negative value also indicates that nanoparticles have high degrees of stability⁵⁰. The negative potential values could also be due to the presence of bio-organic components in the lichen extract that acted as capping agents. Generally, AgNPs synthesized using biological materials has good mono-dispersity as well as stability⁵¹. The particle size differed in TEM and DLS because the principles of the techniques in both analyses were different. The particles size in DLS was larger than those detected by TEM micrographs which could be due to the presence of impurities of bio-active molecules of lichen on the AgNPs surface. In addition to above mentioned points, DLS mainly measures the hydrodynamic radius of the nanoparticles³⁰. The EDS results are consistent with previous studies that reported a strong peak for Xa-AgNPs and Ff-AgNPs at (3 keV), which is typical for the absorption of metallic silver nano-crystallites. Two impurity peaks were detected below 1 keV, which corresponded to carbon peak (CK) and oxygen peak (OK), that might be originated from the lichen extract^{26,28,35}. It is well documented that, lichen extracts contains several metabolites, including antranorin as (+)-praesorediosic acid, and (+)-protopraesorediosic acid that has important roles in the synthesis of AgNPs²⁸. The functional groups of Xa and Ff lichen extracts responsible for the reduction of Ag⁺ from AgNO₃ and stabilization of AgNPs was studied by FTIR³⁰. FTIR is an analytical technique to identify organic and inorganic materials that used to obtain an infrared spectrum of absorption or emission of a solid, liquid and gas²⁹. The spectrum was observed at 3300–3500 cm⁻¹, indicating the presence of polyphenolic –OH group and N–H stretching of amine^{17,25}. On the other hand, it was observed that the ratio between the intensity of the bands at 2066–2070 cm⁻¹ could be attributed to the –C=C– stretch; alkynes⁵². Intense absorption bands in FTIR at 1600–1650 cm⁻¹ might be attributed to amide I due to carbonyl stretch in proteins C=O stretch^{25,27,29,30}. A comparison between the spectra of lichen extracts and AgNPs displayed little alterations in the position and the magnitude of the absorption bands indicating using the lichen secondary metabolites in nanoparticle formation.

Identification of Lichens secondary metabolites by (GC–MS). The efficiency of lichens might be ascribed to a unique chemo-diversity having secondary metabolites 80% more than those produced by other organisms²⁹. In addition, lichens have distinctive chemical compounds that is totally different from those produced by fungi, algae and plants⁵³. At least 1050 different compounds have been identified from lichen species. Such compounds may act as antibacterial, antifungal, antiseptic, anti-inflammatory, antioxidant, antiviral, anticancer and antiproliferative agents as well as healing properties has been also confirmed. However, a major obstacle of lichen metabolites to be incorporated into medical applications is the natural toxicity of some secondary metabolites⁵⁴. In Saudi Arabia, a large number of lichen species are present however, they were not well identified which could be related to the complexity of lichen cultivation. GC–MS results are illustrated in Table 2 displaying similarity with reported literature that detected phenols, amines, aldehydes and ketones, besides many other compounds that could be responsible for the reduction and stabilization of AgNPs^{17,25,30,31}. Lichens of same species may identified different chemical compounds which could be related to substrate types and concentrations that used for lichen extraction⁵⁴. Compared to previous researches, the chemical compounds detected in both lichen types tested in the current study were [undecanal^{55,56}, Piperidine²⁹, and Colchicine⁵⁷]. Benzenamine, 4-methoxy-*N*-methyl-compound was observed in both lichen types of Xa and Ff, it is a form of amine group that possibly contribute in reducing silver ions to AgNPs⁵⁸. Some identified compounds from Xa in the current study had antibacterial activity such as (Benzyl bromide⁵⁹, Hexachlorophene⁶⁰, Pyrrolidine, 1-methyl⁶¹, 2-Amino-2-ethyl-1,3-propanediol⁶², undecanal⁶³). The compounds that has antibacterial activity in Ff lichen are Oxacyclododecan-2-one⁶⁴, Piperidine⁶⁵, Atropine⁶⁶, 2',5'-Dihydroxypropiophenone^{67,68}, and Colchicine⁶⁹. Furthermore, it has also been demonstrated a chemical compound with antioxidant activity in lichen type Xa such

as undecanal⁶³. On the other hand, Oxacyclododecan-2-one⁷⁰, Piperidine⁶⁵, Ricinoleic acid⁷¹, 2',5'-Dihydroxypropiofenone⁶⁸, 2,5-Cyclohexadiene-1,4-dione, 2,6-bis(1,1-dimethylethyl)⁷², and Colchicine⁶⁹ were identified from lichen type Ff and Dichloran⁷³, Hexachlorophene⁷⁴ were found in lichen type Xa, all were characterized by their antifungal activities. Some compounds identified in lichen type Ff showed therapeutic activities such as Beclomethasone that used to treatment of persistent asthma⁷⁵, Colchicine used to treatment of gout⁷⁶, Atropine used to treatment of Arrhythmias⁷⁶ Ff include Beclomethasone⁷⁵ that has anti-inflammatory activity and Octadecylamine⁷⁷ involved with other compounds in materials manufacture that used in drug delivery.

Evaluation of antibacterial activity of AgNPs. Biogenic AgNPs by the aid of both lichens were examined in the current study for antibacterial activity against different bacteria, however, no antibacterial activity was detected for lichen extracts alone; suggesting that 10 mg/mL concentration was not enough for antibacterial efficacy^{26,28–30}. Some investigations reported the antibacterial activity of AgNPs prepared using lichen extracts influenced gram-negative bacteria more than gram-positive bacteria^{26,30,31}; however, our study didn't show the same pattern which is in accordance with some other investigations^{17,28,35}. Noticed activity of the AgNPs against *Pseudomonas aeruginosa*; might be due to the cell wall structure of gram-negative³¹ since MRSA and VRE showed less sensitivity. Penetration of the AgNPs in gram-negative bacteria could be much easier than that in gram-positive due to the cell wall that composed of a thinner layer of peptidoglycan compared to gram-positive²⁸. Ff-AgNPs showed more efficacy against some bacteria strains (MRSA, VRE, *P. aeruginosa* MDR, *E. coli* ATCC) compared to Xa-AgNPs which might be due to the size of the particles that was 69 nm for Ff-AgNPs, while that for Xa-AgNPs was 145 nm. The chemical components were identified from Ff lichen type were more than those identified in Xa which could also be a reason for high antibacterial activity since some of had antibacterial and antioxidant activities. Recent studies have also reported similar trend of observations regarding antibacterial activity of AgNPs against *P. aeruginosa* in relation to *S. aureus* and *E. coli*^{30,31}. *E. coli* in the current study showed less sensitivity to biogenic AgNPs which might be related to the fact that, such antibacterial agents are bacterial specific therefore, AgNPs mechanism against bacteria should be further investigated since no special trend was observed regarding microbial species. It has been noticed that the higher concentration of biogenic AgNPs, the greater the antibacterial activity was detected³⁰. Also, smaller AgNPs with a large surface area possesses antibacterial effects greater than that of larger AgNPs size because the smaller particles can easily anchor to bacterial cell wall and penetrate²⁸. However, several studies proposed that AgNPs mode of action against bacteria could be related to following points (a) interact with the membrane surface during cell wall synthesis (b) suppression during protein synthesis (c) disruption of transcription process (d) perturbation of metabolic pathways where interact of Ag with the thiol groups of respiratory enzymes of bacteria^{17,30}. Furthermore, MICs and MBCs of biogenic AgNPs exhibited good bactericidal activity at low concentrations against tested bacterial strains⁷⁸. No available reports for MICs and MBCs for AgNPs prepared by lichens. The present investigation is in consistence with the other study that revealed the tolerance level was bactericidal for biogenic AgNPs prepared by some plant extracts¹⁶. Synergistic effect of antibiotics and AgNPs was examined and their combination increased the activity against all tested bacterial strains⁷⁹. Tetracycline, linezolid and gentamicin are protein synthesis inhibitors antibiotics. Tetracycline and gentamicin inhibit protein synthesis by binding the 30S subunit of bacterial ribosome, whereas linezolid binds to 50S subunit. Ampicillin is part of beta-lactam antibiotics group and considered as cell wall synthesis inhibitor⁸⁰. Synergistic results represented a significant consensus with previously findings reported the AgNPs using biogenic extracts^{80–85}. Such activity could be of interest to overcome the antibiotic resistant microbes since combination increased the antibiotic activity suggesting easy penetration of the antibiotic active ingredients by the aid of the nanoparticles. Such enhancement of antibiotic activity could be related to the fact that, AgNPs facilitate good transfer to the antibiotic and bind it to the interaction site with the microbe⁸⁶. Same trend of observation was also recorded in various studies⁸⁷.

Cytotoxicity of AgNPs. To investigate the biogenic AgNPs cytotoxicity, MTT test was done against HCT 116, MDA-MB-231 and FaDu cell line that showed high activity since the IC₅₀ was < 100 µg/mL; while MDA-MB-231 was less sensitive and showed IC₅₀ > 100 µg/mL. It has been reported that, biogenically synthesized AgNPs using lichen extracts had anticancer activity against human lung cancer cell line³⁵. In their study, lower IC₅₀ of 3.8 and 6.6 µg/mL were found compared with our results when they used AgNPs synthesized using *Ganoderma lucidum* and *Phellinus igniarius* respectively. Generally, anticancer activity of AgNPs prepared using green synthesis was well documented^{16,35,58,88,89}. Further studies stated the IC₅₀ of AgNPs synthesized using biogenic extract were ranged between 10.9 to 21.4 against HepG2, LoVo, and MDA-MB 231 cell⁹⁰ and another study showed IC₅₀ ranged between 35.15–56.73 µg/mL against a LoVo cell with¹⁶. These differences in cytotoxicity results could be related to cell lines variations and AgNPs size, shape and concentrations. Ff-AgNPs showed more efficacy against all cell lines compared to Xa-AgNPs which might be due to the small size of the particles in Ff-AgNPs. Also, it could be related to the chemical components detected by GC–MS since higher chemicals components were identified from Ff-AgNPs compared to Xa-AgNPs. Differences in sensitivities toward different AgNPs might be due to their physiological behaviour and structural characteristics. Biogenically synthesized AgNPs may inhibit growth of cancer cell lines by various modes of actions. They may cause cellular damage in cancer cell line through the generating of ROS which leads to DNA damage by activation of Caspase-3 molecule, thus undergone apoptosis¹⁷. It could be concluded that, AgNPs may produce free radicals that lead cell oxidative stress, subsequently programmed cell death via caspase cascade pathway⁵⁸.

Conclusion

In the light of our current findings, it might be concluded that methanol extracts of lichen could be potential candidate in reducing and capping of AgNPs in the context of eco-friendly approach for extracellular synthesis in one step. The FTIR analysis showed participation of different lichen biomolecules in reducing and capping of AgNPs. The biogenic AgNPs were well-dispersed spherical of 1–145 nm which was confirmed by TEM and zeta size analysis. The eco-friendly technique presented here might be practical for AgNPs production in large-scale. Encouragingly, the biogenic AgNPs showed promising materials in antibacterial applications against *P. aeruginosa*, MRSA, VRE, and *E. coli*. Additionally, AgNPs influence on gram-negative was greater than that on gram-positive bacteria and higher cytotoxicity against FaDu and HCT 116 cell line in relation to MDA-MB-231 was found. Furthermore, substantial antibacterial and a good synergistic effect for AgNPs when associated with antibiotics might help in antibiotic-resistant microorganism treatment. Therefore, AgNPs prepared in the current study might be recommended for biomedical and pharmaceutical applications. Our study is considered as the first report that studied AgNPs fabricated using lichen types *Xanthoria parietina* and *Flavopunctelia flaventior* and approved their activity and synergistic impact with some antibiotics against pathogenic bacteria as well as cytotoxicity against three cell lines.

Received: 18 July 2020; Accepted: 21 September 2020

Published online: 08 October 2020

References

- Rex, J. H. *et al.* Progress in the fight against multidrug-resistant bacteria 2005–2016: Modern noninferiority trial designs enable antibiotic development in advance of epidemic bacterial resistance. *Arch. Clin. Infect. Dis.* **65**, 141–146. <https://doi.org/10.1093/cid/cix246> (2017).
- WHO. Antimicrobial resistance: global report on surveillance. Report No. 9241564741 (2014).
- Kon, K. & Rai, M. *Antibiotic Resistance: Mechanisms and New Antimicrobial Approaches* 1st edn. (Elsevier Science, Amsterdam, 2016).
- Guillamet, C. V. & Kollef, M. H. “Does this patient have...?” Is this patient at risk for infection with multidrug resistant bacteria?. *Intensive Care Med.* **43**, 436–439. <https://doi.org/10.1007/s00134-015-4126-1> (2017).
- Aliyu, S., Smaldone, A. & Larson, E. Prevalence of multidrug-resistant gram-negative bacteria among nursing home residents: A systematic review and meta-analysis. *Am. J. Infect. Control.* **45**, 512–518. <https://doi.org/10.1016/j.ajic.2017.01.022> (2017).
- Magiorakos, A. P. *et al.* Multidrug-resistant, extensively drug-resistant and pandrug-resistant bacteria: An international expert proposal for interim standard definitions for acquired resistance. *Clin. Microbiol. Infect.* **18**, 268–281. <https://doi.org/10.1111/1/j.1469-0691.2011.03570.x> (2012).
- Cardoso, T., Ribeiro, O., Aragão, I. C., Costa-Pereira, A. & Sarmiento, A. E. Additional risk factors for infection by multidrug-resistant pathogens in healthcare-associated infection: A large cohort study. *BMC Infect. Dis.* **12**, 375. <https://doi.org/10.1186/1471-2334-12-375> (2012).
- Cerceo, E., Deitzelzweig, S. B., Sherman, B. M. & Amin, A. N. Multidrug-resistant gram-negative bacterial infections in the hospital setting: Overview, implications for clinical practice, and emerging treatment options. *Microb. Drug Resist.* **22**, 412–431. <https://doi.org/10.1089/mdr.2015.0220> (2016).
- Rai, M., Deshmukh, S., Ingle, A. & Gade, A. Silver nanoparticles: The powerful nanoweapon against multidrug-resistant bacteria. *J. Appl. Microbiol.* **112**, 841–852. <https://doi.org/10.1111/j.1365-2672.2012.05253.x> (2012).
- Drake, P. L. & Hazelwood, K. J. Exposure-related health effects of silver and silver compounds: A review. *Ann. Occup. Hyg.* **49**, 575–585. <https://doi.org/10.1093/annhyg/mei019> (2005).
- Prabhu, S. & Poulou, E. K. Silver nanoparticles: Mechanism of antimicrobial action, synthesis, medical applications, and toxicity effects. *Int. Nano Lett.* **2**, 32. <https://doi.org/10.1186/2228-5326-2-32> (2012).
- Pal, K. *Hybrid Nanocomposites: Fundamentals, Synthesis, and Applications* (CRC Press, Boca Raton, 2019).
- Pal, K. *Nanofabrication for Smart Nanosensor Applications* (Elsevier, Amsterdam, 2020).
- Jeevanandam, J., Pal, K. & Danquah, M. K. Virus-like nanoparticles as a novel delivery tool in gene therapy. *Biochimie* **157**, 38–47. <https://doi.org/10.1016/j.biochi.2018.11.001> (2019).
- Javed, B., Nadhman, A. & Mashwani, Z.-U.-R. Phytosynthesis of Ag nanoparticles from *Mentha longifolia*: Their structural evaluation and therapeutic potential against HCT116 colon cancer, Leishmanial and bacterial cells. *Appl. Nanosci.* <https://doi.org/10.1007/s13204-020-01428-5> (2020).
- Mohammed, A., Al-Qahtani, A., Al-Mutairi, A., Al-Shamri, B. & Aabed, K. Antibacterial and cytotoxic potential of biosynthesized silver nanoparticles by some plant extracts. *Nanomaterials* **8**, 382. <https://doi.org/10.3390/nano8060382> (2018).
- Siddiqi, K. S., Rashid, M., Rahman, A., Husen, A. & Rehman, S. Biogenic fabrication and characterization of silver nanoparticles using aqueous-ethanolic extract of lichen (*Usnea longissima*) and their antimicrobial activity. *Biomater. Res.* **22**, 23. <https://doi.org/10.1186/s40824-018-0135-9> (2018).
- Alavi, M. & Rai, M. Recent progress in nanoformulations of silver nanoparticles with cellulose, chitosan, and alginate biopolymers for antibacterial applications. *Appl. Microbiol. Biotechnol.* **103**, 8669–8676. <https://doi.org/10.1007/s00253-019-10126-4> (2019).
- Friedman, A. J. *et al.* Antimicrobial and anti-inflammatory activity of chitosan-alginate nanoparticles: A targeted therapy for cutaneous pathogens. *J. Investig. Dermatol.* **133**, 1231–1239. <https://doi.org/10.1038/jid.2012.399> (2013).
- Herrera, M., Carrión, P., Baca, P., Liébana, J. & Castillo, A. In vitro antibacterial activity of glass-ionomer cements. *Microbios* **104**, 141–148 (2001).
- Ahmed, S., Ahmad, M., Swami, B. L. & Ikram, S. A review on plants extract mediated synthesis of silver nanoparticles for antimicrobial applications: A green expertise. *J. Adv. Res.* **7**, 17–28. <https://doi.org/10.1016/j.jare.2015.02.007> (2016).
- Iravani, S. Green synthesis of metal nanoparticles using plants. *Green Chem.* **13**, 2638–2650. <https://doi.org/10.1039/C1GC15386B> (2011).
- Mastan, A., Sreedevi, B. & Kumari, J. P. Evaluation of the in vitro antioxidant and antibacterial activities of secondary metabolites produced from lichens. *Asian J. Pharm. Clin. Res.* **7**, 193–198 (2014).
- Kambar, Y., Vivek, M., Manasa, M. & Mallikarjun, N. Antimicrobial activity of *Leptogium burnetiae*, *Ramalina hossei*, *Roccella montagnei* and *Heterodermia diademata*. *Int. J. Pharm. Phytopharm. Res.* **4**, 164–168 (2014).
- Dasari, S. *et al.* Biosynthesis, characterization, antibacterial and antioxidant activity of silver nanoparticles produced by lichens. *J. Bionanosci.* **7**, 237. <https://doi.org/10.1166/jbns.2013.1140> (2013).
- Mie, R. *et al.* Synthesis of silver nanoparticles with antibacterial activity using the lichen *Parmotrema praesorediosum*. *Int. J. Nanomed.* **9**, 121–127. <https://doi.org/10.2147/IJN.S52306> (2014).

27. Yıldız, N. *et al.* Investigation of lichen based green synthesis of silver nanoparticles with response surface methodology. *Green Process. Synth.* **3**, 259–270. <https://doi.org/10.1515/gps-2014-0024> (2014).
28. Din, L. B., Mie, R., Samsudin, M. W., Ahmad, A. & Ibrahim, N. Biomimetic synthesis of silver nanoparticles using the lichen *Ramalina dumeticola* and the antibacterial activity. *Malays. J. Anal. Sci.* **19**, 369–376 (2015).
29. Leela, K. & Anchana, D. C. A study on the applications of silver nanoparticle synthesized using the aqueous extract and the purified secondary metabolites of Lichen *Parmelia perlata*. *Int. J. Pharm. Sci. Invent.* **6**, 42–59 (2017).
30. Khandel, P., Shahi, S. K., Kanwar, L., Yadaw, R. K. & Soni, D. K. Biochemical profiling of microbes inhibiting silver nanoparticles using symbiotic organisms. *Int. J. Pharm. Sci. Invent.* **9**, 273–285 (2018).
31. Rai, H. & Gupta, R. K. Biogenic fabrication, characterization, and assessment of antibacterial activity of silver nanoparticles of a high altitude Himalayan lichen—*Cladonia rangiferina* (L.) Weber ex FH Wigg. *Trop. Plant Res.* **6**, 293–298. <https://doi.org/10.22271/tpr.2019.v6.i2.037> (2019).
32. Nayaka, S. Methods and techniques in collection, preservation and identification of lichens. In *Plant Toxon. Biosystema. Class Mod. Meth.* (eds Nair, K. N., Rana, T. S., Upreti, D.K.) Ch. 5, 101–128 (New India Publishing Agency, New Delhi, 2014).
33. Ghazanfar, S. A. & Fisher, M. *Vegetation of the Arabian Peninsula* Vol. 25 (Springer Science & Business Media, New York, 2013).
34. Kumar, S. P., Kekuda, T. P., Vinayaka, K. & Yogesh, M. Synergistic efficacy of lichen extracts and silver nanoparticles against bacteria causing food poisoning. *Asian J. Res. Chem.* **3**, 67–70 (2010).
35. Paul, S., Singh, A. R. & Sasikumar, C. S. Green synthesis of bio-silver nanoparticles by *Parmelia perlata*, *Ganoderma lucidum* and *Phellinus igniarius* & their fields of application. *Indian J. Res. Pharm Biotechnol.* **3**, 100 (2015).
36. Mitrovic, T. *et al.* *Platismatia glauca* and *Pseudevernia furfuracea* lichens as sources of antioxidant, antimicrobial and antibiofilm agents. *Exp. Clin. Sci.* **13**, 938 (2014).
37. Sundararaj, J. P., Kuppuraj, S., Ganesan, A., Ponnusamy, P. & Nayaka, S. In vitro assessment of antioxidant and antimicrobial activities of different solvent extracts from lichen *Ramalina nervulosa*. *Int. J. Pharm. Pharm. Sci.* **7**, 200–204 (2015).
38. CLSI. M100: performance standards for antimicrobial susceptibility testing. Report No. 1-56238-838-X (Clinical and Laboratory Standards Institute, Wayne, 2018).
39. CLSI. M02: Performance standards for antimicrobial disk susceptibility tests. Report No. 1-56238-834-7 (Clinical and Laboratory Standards Institute, Wayne, 2018).
40. CLSI. M07: Methods for dilution antimicrobial susceptibility tests for bacteria that grow aerobically. Report No. 1-56238-836-3 (Clinical and Laboratory Standards Institute, Wayne, 2018).
41. Basri, D. F. & Fan, S. The potential of aqueous and acetone extracts of galls of *Quercus infectoria* as antibacterial agents. *Indian J. Pharm.* **37**, 26. <https://doi.org/10.4103/0253-7613.13851> (2005).
42. Jyoti, K., Baunthiyal, M. & Singh, A. Characterization of silver nanoparticles synthesized using *Urtica dioica* Linn. leaves and their synergistic effects with antibiotics. *J. Radiat. Res. Appl. Sci.* **9**, 217–227. <https://doi.org/10.1016/j.jrras.2015.10.002> (2015).
43. Mosmann, T. Rapid colorimetric assay for cellular growth and survival: Application to proliferation and cytotoxicity assays. *J. Immunol. Methods* **65**, 55–63. [https://doi.org/10.1016/0022-1759\(83\)90303-4](https://doi.org/10.1016/0022-1759(83)90303-4) (1983).
44. Cole, S. Rapid chemosensitivity testing of human lung tumor cells using the MTT assay. *Cancer Chemother. Pharmacol.* **17**, 259–263. <https://doi.org/10.1007/BF00256695> (1986).
45. Alshammari, B. A. *et al.* Characterization of the viscoelastic, dielectric, and biological behavior of porous polyethylene for hard tissue replacement. *Sci Adv. Mater.* **9**, 2073–2081. <https://doi.org/10.1166/sam.2017.3236> (2017).
46. Alqahtani, M. A., Mohammed, A. E., Daoud, S. I., Alkhalifah, D. H. M. & Albrahim, J. S. Lichens (*Parmotrema clavuliferum*) extracts: Bio-mediator in silver nanoparticles formation and antibacterial potential. *J. Bionanosci.* **11**, 410–415. <https://doi.org/10.1166/jbns.2017.1457> (2017).
47. Siddiqi, K. S., Husen, A. & Rao, R. A. A review on biosynthesis of silver nanoparticles and their biocidal properties. *J. Nanobiotechnol.* **16**, 14. <https://doi.org/10.1186/s12951-018-0334-5> (2018).
48. Lee, S. H. & Jun, B.-H. Silver nanoparticles: Synthesis and application for nanomedicine. *Int. J. Mol. Sci.* **20**, 865. <https://doi.org/10.3390/ijms20040865> (2019).
49. Guilger-Casagrande, M. & de Lima, R. Synthesis of silver nanoparticles mediated by fungi: A review. *Front. Bioeng. Biotechnol.* **7**, 287. <https://doi.org/10.3389/fbioe.2019.00287> (2019).
50. Béteky, P. *et al.* Silver nanoparticles: Aggregation behavior in biorelevant conditions and its impact on biological activity. *Int. J. Nanomed.* **14**, 667. <https://doi.org/10.2147/IJN.S185965> (2019).
51. Irvani, S., Korbekandi, H., Mirmohammadi, S. V. & Zolfaghari, B. Synthesis of silver nanoparticles: Chemical, physical and biological methods. *Res. Pharm. Sci.* **9**, 385–406 (2014).
52. Chanthini, A. B. *et al.* Structural characterization, antioxidant and in vitro cytotoxic properties of seagrass, *Cymodocea serrulata* (R. Br.) Asch. & Magnus mediated silver nanoparticles. *J. Photochem. Photobiol. B.* **153**, 145–152. <https://doi.org/10.1016/j.jphotobiol.2015.09.014> (2015).
53. Lokajová, V., Bačkorová, M. & Bačkor, M. Allelopathic effects of lichen secondary metabolites and their naturally occurring mixtures on cultures of aposymbiotically grown lichen photobiont *Trebouxia erici* (Chlorophyta). *S. Afr. J. Bot.* **93**, 86–91. <https://doi.org/10.1016/j.sajb.2014.03.015> (2014).
54. Letwin, L. S. *Biological Activities of Select North American Lichens*, Master thesis, Lakehead University (2017).
55. Joulain, D. & Tabacchi, R. Lichen extracts as raw materials in perfumery. Part 1: oakmoss. *Flavour Frag. J.* **24**, 49–61. <https://doi.org/10.1002/ffj.1916> (2009).
56. Chahra, D., Ramdani, M., Lograda, T., Chalard, P. & Figueredo, G. Chemical composition and antimicrobial activity of *Evernia prunastri* and *Ramalina farinacea* from Algeria. *Issues Biol. Sci. Pharm. Res.* **4**, 35–42. <https://doi.org/10.15739/ibspr.16.005> (2016).
57. Gopinath, K., Gowri, S., Karthika, V. & Arumugam, A. Green synthesis of gold nanoparticles from fruit extract of *Terminalia arjuna*, for the enhanced seed germination activity of *Gloriosa superba*. *J. Nanostructure Chem.* **4**, 115. <https://doi.org/10.1007/s40097-014-0115-0> (2014).
58. Jeyaraj, M. *et al.* Biogenic silver nanoparticles for cancer treatment: An experimental report. *Colloids Surf. B.* **106**, 86–92. <https://doi.org/10.1016/j.colsurfb.2013.01.027> (2013).
59. Shakhatreh, M. A. K. *et al.* Study of the antibacterial and antifungal activities of synthetic benzyl bromides, ketones, and corresponding chalcone derivatives. *Drug Des. Dev. Ther.* **10**, 3653–3660. <https://doi.org/10.2147/DDDT.S116312> (2016).
60. Miller, L. G., Tan, J., Eells, S. J., Benitez, E. & Radner, A. B. Prospective investigation of nasal mupirocin, hexachlorophene body wash, and systemic antibiotics for prevention of recurrent community-associated methicillin-resistant *Staphylococcus aureus* infections. *Antimicrob. Agents Chemother.* **56**, 1084–1086. <https://doi.org/10.1128/aac.01608-10> (2012).
61. Rajakumar, P., Thirunarayanan, A. & Raja, S. Synthesis and antibacterial activity of novel N-methyl pyrrolidine dendrimers via [3+ 2] cycloaddition. *Proc. Natl. Acad. Sci. India A.* **84**, 371–379. <https://doi.org/10.1007/s40010-013-0120-6> (2014).
62. Venugopal, K. *et al.* Chemical synthesis, characterization and antibacterial activity of 2-amino-2-ethyl 1, 3 propanediol and its Cu (II), Ru (II) complexes. *Unique Res. J. Chem.* **2**, 8–15 (2014).
63. Hassim, N. *et al.* Antioxidant and antibacterial assays on polygonum minus extracts: Different extraction methods. *Int. J. Chem. Eng.* <https://doi.org/10.1155/2015/826709> (2015).
64. Raval, S., Vaghela, P. G., Mandavia, M. & Golakiya, B. A. Phytochemical analysis of *Malaxis acuminata* D. Don (Jeevak), an ingredient of Jeevaniya Group of Ashtavarga. *Indian J. Agric. Biochem.* **29**, 155–160. <https://doi.org/10.5958/0974-4479.2016.00025.3> (2016).

65. Naicker, L., Venugopala, K., Shode, F. & Odhav, B. Antimicrobial and antioxidant activities of piperidine derivatives. *Afr. J. Pharm. Pharmacol.* **9**, 783–792. <https://doi.org/10.5897/AJPP2015.4335> (2015).
66. Ittzes, B., Weiling, Z., Batai, I., Kerenyi, M. & Batai, I. Atropine and glycopyrrolate do not support bacterial growth—safety and economic considerations. *J. Clin. Anesth.* **35**, 560–563. <https://doi.org/10.1016/j.jclinane.2016.09.011> (2016).
67. Sumsakul, W. & Na-Bangchang, K. In vitro and in vivo antibacterial activities of 1, 4-naphthoquinone derivatives in silkworm model. *R. Thai Army Med. J.* **67**, 155–162 (2014).
68. Prasanna, R., Nandhini, B., Praveesh, B. V., Jayaraman, A. & Muthusamy, P. Novel angiotensin converting enzyme inhibitor from *Aspergillus* SP. by solid state fermentation. *Int. J. Pharm. Pharm. Sci* **4**, 371–377 (2012).
69. Huczynski, A. *et al.* Synthesis, antiproliferative and antibacterial evaluation of C-ring modified colchicine analogues. *Eur. J. Med. Chem.* **90**, 296–301. <https://doi.org/10.1016/j.ejmech.2014.11.037> (2015).
70. Kadhim, M. J., Mohammed, G. J. & Hameed, I. H. In vitro antibacterial, antifungal and phytochemical analysis of methanolic extract of fruit *Cassia fistula*. *Orient. J. Chem.* **32**, 1329. <https://doi.org/10.13005/ojc/320307> (2016).
71. Oloyede, G. Antioxidant activities of methyl ricinoleate and ricinoleic acid dominated ricinus communis seeds extract using lipid peroxidation and free radical scavenging methods. *J. Med. Plant Res.* **6**, 511–520. <https://doi.org/10.3923/rjmp.2012.511.520> (2012).
72. Liu, R., Song, S., Lin, Y., Ruan, T. & Jiang, G. Occurrence of synthetic phenolic antioxidants and major metabolites in municipal sewage sludge in China. *Environ. Sci. Technol.* **49**, 2073–2080. <https://doi.org/10.1021/es505136k> (2015).
73. Henson, O. Dichloran as an inhibitor of mold spreading in fungal plating media: Effects on colony diameter and enumeration. *Appl. Environ. Microbiol.* **42**, 656–660. <https://doi.org/10.1128/AEM.42.4.656-660.1981> (1981).
74. Mello, T. *et al.* Drug repurposing strategy against fungal biofilms. *Curr. Top. Med. Chem.* <https://doi.org/10.2174/156802662007200316142626> (2020).
75. Terakosolphan, W., Altharawi, A., Chan, K. L. & Forbes, B. Quantification of beclomethasone dipropionate in living respiratory epithelial cells using Infrared Spectroscopy. *J. Aerosol. Med. Pulm. D.* **32**, A22–A22 (2019).
76. Slobodnick, A., Shah, B., Pillinger, M. & Krasnokutsky, S. Colchicine: Old and new. *Am. J. Med. Sci.* **128**, 461–470. <https://doi.org/10.1016/j.amjmed.2014.12.010> (2015).
77. Georgiadou, V., Makris, G., Papagiannopoulou, D., Vourlias, G. & Dendrinou-Samara, C. Octadecylamine-mediated versatile coating of CoFe₂O₄ NPs for the sustained release of anti-inflammatory drug naproxen and in vivo target selectivity. *ACS Appl. Mater. Interfaces.* **8**, 9345–9360. <https://doi.org/10.1021/acsami.6b00408> (2016).
78. Moteriya, P. & Chanda, S. Biosynthesis of silver nanoparticles formation from *Caesalpinia pulcherrima* stem metabolites and their broad spectrum biological activities. *J. Genet. Eng. Biotechnol.* **16**, 105–113. <https://doi.org/10.1016/j.jgeb.2017.12.003> (2018).
79. Katva, S., Das, S., Moti, H. S., Jyoti, A. & Kaushik, S. Antibacterial synergy of silver nanoparticles with gentamicin and chloramphenicol against *Enterococcus faecalis*. *Pharm. Mag.* **13**, S828–S833. https://doi.org/10.4103/pm.pm_120_17 (2017).
80. Kohanski, M. A., Dwyer, D. J. & Collins, J. J. How antibiotics kill bacteria: From targets to networks. *Nat. Rev. Microbiol.* **8**, 423–435. <https://doi.org/10.1038/nrmicro2333> (2010).
81. McShan, D., Zhang, Y., Deng, H., Ray, P. C. & Yu, H. Synergistic antibacterial effect of silver nanoparticles combined with ineffective antibiotics on drug resistant *Salmonella typhimurium* DT104. *J. Environ. Sci. Health C.* **33**, 369–384. <https://doi.org/10.1080/10590590.2015.1055165> (2015).
82. Wan, G. *et al.* Effects of silver nanoparticles in combination with antibiotics on the resistant bacteria *Acinetobacter baumannii*. *Int. J. Nanomed.* **11**, 3789–3800. <https://doi.org/10.2147/IJN.S104166> (2016).
83. Jamaran, S. & Zarif, B. R. Synergistic effect of silver nanoparticles with neomycin or gentamicin antibiotics on mastitis-causing *Staphylococcus aureus*. *Open J. Ecol.* **6**, 452–459. <https://doi.org/10.4236/oje.2016.67043> (2016).
84. Tawfeeq, S. M., Maarroof, M. N. & Al-Ogaidi, I. Synergistic effect of biosynthesized silver nanoparticles with antibiotics against multi-drug resistance bacteria isolated from children with diarrhoea under five years. *Iraqi J. Sci.* **58**, 41–52 (2017).
85. Krychowiak, M., Kawiak, A., Narajczyk, M., Borowik, A. & Króllicka, A. Silver nanoparticles combined with naphthoquinones as an effective synergistic strategy against *Staphylococcus aureus*. *Front. Pharmacol.* **9**, 816. <https://doi.org/10.3389/fphar.2018.00816> (2018).
86. Allahverdiyev, A. M., Kon, K. V., Abamor, E. S., Bagirova, M. & Rafailovich, M. Coping with antibiotic resistance: Combining nanoparticles with antibiotics and other antimicrobial agents. *Expert Rev. Anti-infect. Ther.* **9**, 1035–1052. <https://doi.org/10.1586/eri.11.121> (2011).
87. Sharma, N., Jandaik, S. & Kumar, S. Synergistic activity of doped zinc oxide nanoparticles with antibiotics: Ciprofloxacin, ampicillin, fluconazole and amphotericin B against pathogenic microorganisms. *An. Acad. Bras. Ciênc.* **88**, 1689–1698. <https://doi.org/10.1590/0001-3765201620150713> (2016).
88. Al-Sheddi, E. *et al.* Anticancer potential of green synthesized silver nanoparticles using extract of *Nepeta deflersiana* against human cervical cancer cells (HeLa). *Bioinorg. Chem. Appl.* **1–12**, 2018. <https://doi.org/10.1155/2018/9390784> (2018).
89. Al-Brahim, J. S. & Mohammed, A. E. Antioxidant, cytotoxic and antibacterial potentials of biosynthesized silver nanoparticles using bee's honey from two different floral sources in Saudi Arabia. *Saudi J. Biol. Sci.* **27**, 363–373. <https://doi.org/10.1016/j.sjbs.2019.10.006> (2020).
90. Algebaly, A. S., Mohammed, A. E., Abutaha, N. & Elobeid, M. M. Biogenic synthesis of silver nanoparticles: Antibacterial and cytotoxic potential. *Saudi J. Biol. Sci.* **27**, 1340–1351. <https://doi.org/10.1016/j.sjbs.2019.12.014> (2020).

Acknowledgements

Author is grateful to the King Abdulaziz City for Science and Technology (KACST) who provided financial support under the Grant No 1-17-01-001-0058 for this study.

Author contributions

M.A, M.O and A.M. designed the experiments. M.A performed the experiment, statistical analysis and presented the results under direct supervision of A.M. Furthermore, M.A. and A.M. interpreted the data and contributed to writing up the paper. Authors approved manuscript for publishing.

Competing interests

The authors declare no competing interests.

Additional information

Correspondence and requests for materials should be addressed to A.E.M.

Reprints and permissions information is available at www.nature.com/reprints.

Publisher's note Springer Nature remains neutral with regard to jurisdictional claims in published maps and institutional affiliations.



Open Access This article is licensed under a Creative Commons Attribution 4.0 International License, which permits use, sharing, adaptation, distribution and reproduction in any medium or format, as long as you give appropriate credit to the original author(s) and the source, provide a link to the Creative Commons licence, and indicate if changes were made. The images or other third party material in this article are included in the article's Creative Commons licence, unless indicated otherwise in a credit line to the material. If material is not included in the article's Creative Commons licence and your intended use is not permitted by statutory regulation or exceeds the permitted use, you will need to obtain permission directly from the copyright holder. To view a copy of this licence, visit <http://creativecommons.org/licenses/by/4.0/>.

© The Author(s) 2020